Results from the First Deployment of the BASS Rake Field Prototype

Archie T. Morrison III

Department of Applied Ocean Physics and Engineering
Woods Hole Oceanographic Institution
Woods Hole, Massachusetts 02543

Abstract - **The BASS Rake is an acoustic travel time current meter designed to make spatially and temporally dense velocity profile measurements in the continental shelf wave bottom boundary layer. The thinness of the layer is responsible for high levels of bottom shear stress which are important contributors to the sediment entrainment process and which enhance turbulent dissipation of flow energy. The BASS Rake is a modification of BASS, the Benthic Acoustic Stress Sensor, using a new geometry to image flow in the WBBL. A laboratory prototype has previously demonstrated the features and near bed capabilities of the new design. The field prototype described here was constructed with standard BASS components to evaluate the measurement technique and the performance of the support frame in the near shore zone. The field prototype measures the horizontal velocity vector at ten heights from the bottom up to 30 cm above the bottom. The results of tow tank calibration and cosine response measurements are presented. After calibration the field prototype was deployed in 3 m of water immediately outside the surf zone of a local beach. Profiles were recorded continuously at 1 Hz for approximately 3.5 weeks in December of 1996. This period includes both calm and storm conditions. Selected data from this deployment are presented.**

I. INTRODUCTION

The BASS Rake wave bottom boundary layer sensor has been under development at the Woods Hole Oceanographic Institution (WHOI) during the past three years. Most aspects of the design have now been evaluated and proven using a series of laboratory and field capable prototypes. The important features of the mechanical and electronic designs are documented in [2], [3], and [4] and the initial calibration and testing of the laboratory prototype is described in [5]. The definitive description of the development and use of the BASS Rake, to date, can be found in [6].

A portion of the work done on and with the BASS Rake field prototype is documented in this paper. This instrument uses standard BASS components, rather than the more ambitious design described in the references listed above. The field prototype was constructed to demonstrate the operation of this measurement technique in the field, to evaluate the support frame for stability and diver access, and to obtain measurements of near bottom flow and evolving bottom morphology for use in the final stages of the instrument design process. The prototype has successfully accomplished these tasks, returning an extensive and useful data set and providing the author and others involved in the development a great wealth of practical experience.

The field prototype is briefly described in Section II. Section III presents the results of an empirical determination of the sensor response, a function of the magnitude and angle of the flow. Selected data from a 3.5 week deployment outside the surf zone of a local beach are presented in Section IV.

This work was supported by AASERT funding under ONR grant N00014-96-1-0953. WHOI Contribution No. 9497.

II. DESCRIPTION OF THE PROTOTYPE

The BASS Rake field prototype is shown in Figure 1. The instrument consists of a rigid outer frame constructed of aluminum tubing. The outer frame supports an inner frame, mounted on vertical sliders. The electronics housing, the coaxial transmission lines, and the tine assemblies of the BASS Rake are mounted on the inner frame. This construction permits vertical adjustment of the sensor head without loss of the calibrated zero offsets due to relative motions of the electronics housing, transmission line harness, and transducers [6, 7]. The inner assembly and the sliders can be cleanly separated as a rigid unit from the outer frame without disrupting the harness. This feature was necessary for the tow tank determination of the sensor response described in Section III.

The overall assembly has been kept small and light for deployment from small boats or by divers. The cross-braced box frame securing the tops of the four legs prevents significant flexure and the pyramidal members above the box frame support the lift point and protect the pressure housing. The overall weight in air, inclusive of the electronics package, is 300 *lbs* to 350 *lbs*. The in-water weight is 150 *lbs* to 200 *lbs*. Four divers were sufficient to load the instrument on and off a flatbed truck and to deploy and recover it from a beach. The winch and boom of a small boat would also be sufficient. The open design of the frame, the long tines, and the vertical orientation of the single pressure housing are all intended to decrease the flow disturbance in the wave boundary layer and to permit clear access to divers.

The sensor head is shown in Figure 2. Molded polyurethane tranducer assemblies [7] are bolted to the tines to measure the horizontal velocity at ten heights, denoted Level 0 through Level 9 from bottom to top. Levels 0 to 8 are linearly spaced, with a 2.5 *cm* vertical separation, and extend over 20 *cm* vertically. Level 9 is located 10 *cm* above the top of the linear portion of

0-7803-4108-2/97/$10.00 ©1997 IEEE

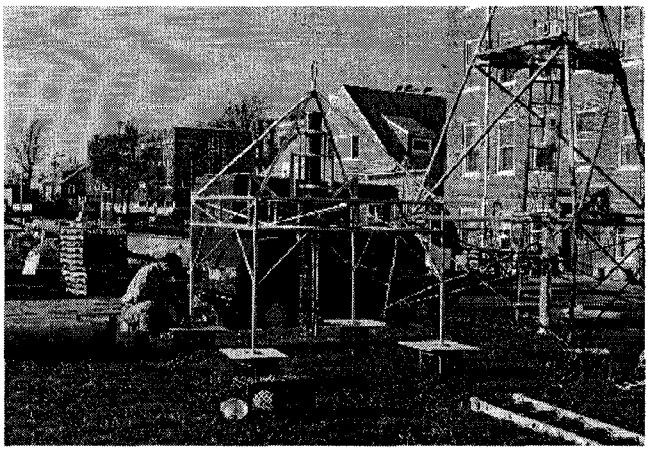

Figure 1. BASS RAKE FIELD PROTOTYPE - The rigid outer frame is constructed of aluminum tubing. The legs are arranged in a square with $2\,m$ sides. The height at the top of the box frame is $1.4\,m$ and the height at the lift point is $2.75\,m$. The pyramidal members above the box frame support the lift point and protect the pressure housing. The housing, mounted vertically in the center of the frame, contains the BASS electronics package, the data logger, and batteries. The tine assemblies extend down from the pressure housing with the sensing volumes at the lower end. The quadrapod designer has been included for scale. Photograph by the author.

the array. The tine members are $\frac{3}{8}''$ square stainless steel solid rod stock. Their overall length below the box frame is $1\,m$. The tines extend $5\,cm$ below the lowermost measurement level and are secured at that point to a ring. The ring suppresses relative motions of the tines and maintains the $15\,cm$ path length separation of the transducers. During deployment the ring is buried in the sediment and the bottom sensor level is at or below the fluid-sediment interface. Further discussion of these and other features of the sensor head can be found in [6].

III. FLOW DISTORTION AND TOW TANK CALIBRATION

Clearly, there will be some flow disturbance associated with the physical intrusion of the sensor head into the boundary layer flow. It can be shown by calculation that the measured velocity will be 5 % to 10 % low for small azimuthal rotation angles.[1] Further, the error will increase with rotation angle up to 45° and be mirrored in each subsequent octant because of symmetry. The simple model on which the calculation is based suggests that the magnitude of the error is also a function of the Reynolds number and possibly of the Keulegan-Carpenter number in the oscillatory boundary layers the BASS Rake is intended to profile [5, 6].

The actual response was empirically determined in a tow tank by comparing the known and measured magnitudes of the velocity over ranges of both the tow cart speed and the azimuthal rotation angle. The gain correction is defined by

$$G_{corr} = \frac{u_{cart}}{u_{m_{at}}} \tag{1}$$

where u_{cart} is the known tow cart speed and $u_{m_{at}}$ is the measured along-tank velocity. The anticipated dependence of G_{corr} on both the magnitude and the angle of the flow was confirmed by this procedure and is shown in Table I and Figure 3. The values given were determined for steady flow, but are accurate in oscillatory flows over the expected range of the Keulegan-Carpenter number of the BASS Rake in the continental shelf wave bottom boundary layer.

Tow Speed	Rotation Angle			
$[cm \cdot s^{-1}]$	0°	15°	30°	45°
1.2	1.12	1.23	1.56	4.33
5	1.07	1.15	1.44	3.69
10	1.06	1.12	1.41	3.29
20	1.04	1.09	1.36	3.04
35	1.04	1.09	1.35	3.02
50	1.04	1.09	1.36	3.02

Table I

GAIN CORRECTION AS A FUNCTION OF TOW SPEED AND ROTATION ANGLE - The gain correction is defined by Equation 1. The dependence on the magnitude of the velocity is essentially flat beyond $10\,cm \cdot s^{-1}$. The angular dependence is strong at all speeds. The response of the sensor for angles below 30° is relatively flat and the required correction is not excessive. For angles near 45° the correction is repeatable, but too large to preserve great measurement accuracy. In agreement with prediction, the measured velocity at small angles is low by less than 10 %.

The response is well behaved and relatively flat out to an angle of at least 30° and the magnitude of the correction in this region is not excessive. For angles near 45° the correction is repeatable, but the level of wake noise is high and the correction is too large to preserve great measurement accuracy. It is, of course, possible to remove or ignore velocities with angles near 45° when processing the data. This did not prove necessary in the analysis of the field data described in Section IV. The instrument was aligned with the shore and velocity angles were consistently within 20° of zero.

Processing requires only a straightforward application of the gain correction to the velocity measurements. The correction is simply formulated as a single-valued mapping from u_m, the measured velocity, to u_{gc}, the corrected or undisturbed velocity. The standard deviation of the error surface associated with the mapping is less than $0.2\,cm \cdot s^{-1}$. This is the effective noise floor of the field prototype. The noise floor of the final instrument is expected to be smaller. A broader and more detailed discussion of the sensor response and its implications can be found in [6].

IV. SELECTED DATA FROM THE DEPLOYMENT

The field prototype was deployed outside the surf zone of Nobska Beach, located approximately $1\,Km$ from WHOI, from December 7 through December 31, 1996. The beach is on a shallow bay and faces SSW down Vineyard Sound. This is the direction of longest fetch and swell commonly

[1] The rotation angle is defined to be 0° when the flow is aligned with two parallel sides of the square formed by the tines and perpendicular to the remaining sides. The rotation angle is 45° when the flow is parallel to one diagonal and perpendicular to the other.

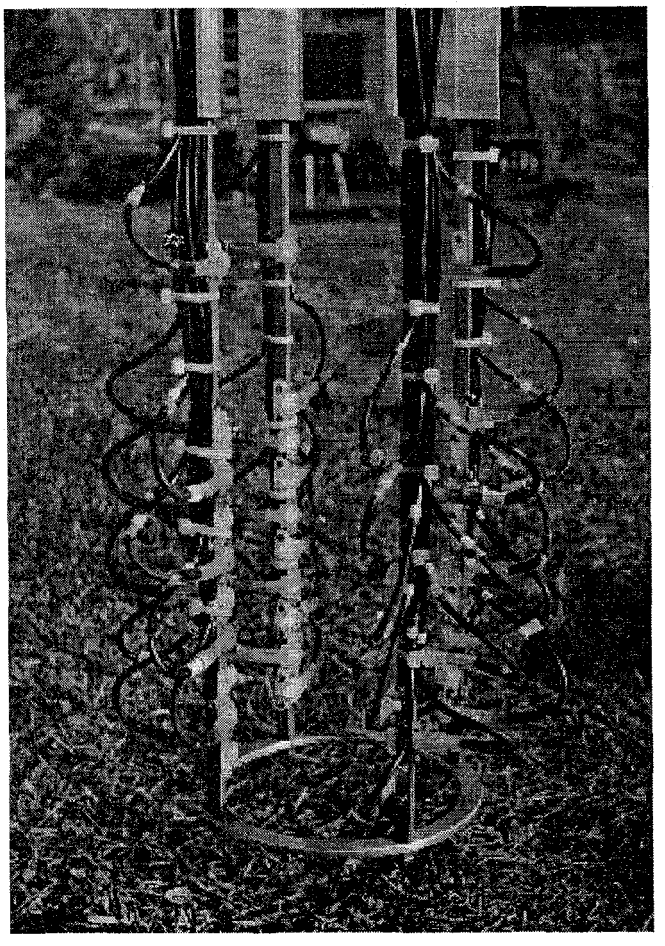

Figure 2. FIELD PROTOTYPE SENSOR HEAD - The molded polyurethane BASS transducer assemblies are bolted to the stainless steel tine members. There are ten measurement levels. The lower nine levels are linearly spaced with a vertical separation of 2.5 cm. The coaxial transmission lines are run along the tines and the angle stock stiffeners and secured with tie-wraps. The structural ring is visible, bolted to the ends of the tines. Photograph by the author.

propagates NNE towards the beach. Great Ledge, a shallow shoal 0.75 Km off-shore tends to attenuate the swell before it reaches the beach. The flood and ebb tidal currents flow parallel to the beach and can reach speeds in excess of 3 kts in the channel beyond Great Ledge. The flood current is towards the east and the ebb towards the west. The near-bottom measurements reported below show that on-shore wave velocities are strongly enhanced during the flood tide. One possible explanation is refraction of the swell around the attenuating shallows and onto the beach by tidal currents during the flood.

The coordinate system used here defines velocities perpendicular to the beach, u_{ogc}, to be positive towards the shore. Along-shore velocities, u_{agc}, are defined postitve towards the WNW, 90° CCW from the shoreward direction. In addition to indicating the on-shore or along-shore direction, the subscripts indicate that these reported velocities have been corrected for the flow distubance of the sensor head, as discussed in Section III.

The deployment site is an open sand patch 5 m to 8 m across in all directions. The water depth is approxi-

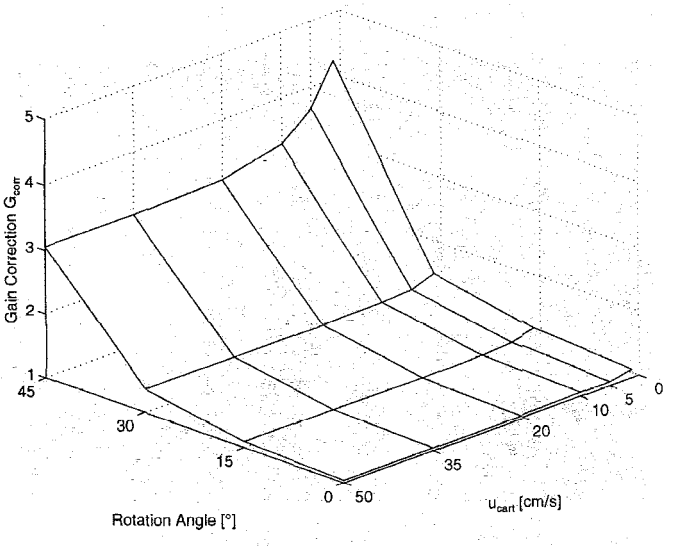

Figure 3. GAIN CORRECTION SURFACE AS A FUNCTION OF TOW SPEED AND ROTATION ANGLE - The gain correction at each point of the grid is calculated using Equation 1. The response of the sensor for angles below 30° is relatively flat and the required correction is not excessive. For angles near 45° the correction is repeatable, but too large to preserve great measurement accuracy. The surface is used to define a single-valued mapping from the measured velocity to the undisturbed velocity.

mately 3 m. A regular pattern of sand ripples was observed on each of the four occasions that the site was visited by divers in November and December of 1996. Those observations bracket the experiment. The BASS Rake measurements show that the bed was reworked over the course of the experiment and are consistent with the persistent presence of dynamically changing sand ripples. This appears to be the normal condition of the site. The ripples are symmetric, indicating generation by waves rather than currents. Ripple wavelengths are 25 cm to 30 cm, with heights of 5 cm to 8 cm. Wave forcing during late November and early December was fairly mild. The velocity measurements indicate greater ripple height during storm events in mid and late December.

The sand ripples were smoothed away in the immediate vicinity of the transducer array during the insertion of the structural ring and tines into the bottom. The lowermost measurement level was placed approximately 1 cm above the smoothed fluid-sediment interface. A storm late on the night of the deployment reworked the bed, raising sand ripples of sufficient height to obscured the bottom three measurement heights (Levels 0 to 2). This condition persisted for most of the deployment. It should be noted that interpretations of the BASS Rake velocity record indicating sediment movement and bedform generation or modification were always consistent with calculations of the Shields parameter and with the wave-current boundary layer model of Grant and Madsen [1, 6]. A more complete discussion of bed evolution during the deployment can be found in [6].

A. *Tidal Modulation of Sediment Transport*

A tidal signature is clearly evident throughout the data set. As noted above, near-bottom wave velocities are consistently and strongly enhanced during the flood tide. This characteristic of the flow is shown in Figures 4 and 5

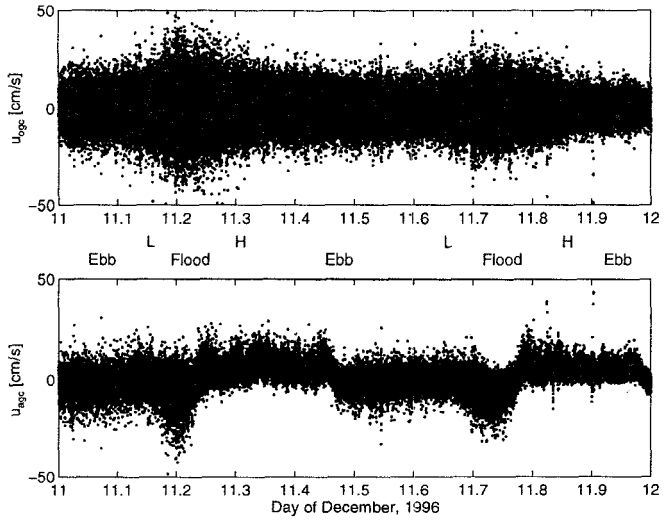

Figure 4. VELOCITY MEASUREMENTS AT LEVEL 3 FOR DECEMBER 11, 1996 - The two panels show the on-shore and along-shore velocities sampled at 1 Hz approximately 2 cm above the crest of a sand ripple estimated to be 5 cm to 6 cm in height. The horizontal scale extends for 24 hours, from midnight to midnight. 11.5 on the scale is noon of December 11, 1996. The state of the tide is marked on the strip between the panels. "H" and "L" mark the approximate times of high and low water at Little Harbor, adjacent to Nobska Beach. The periods of flood and ebb are also marked. Clearly the on-shore wave velocities increase during the flood tide and a semi-diurnal variation of this characteristic is evident. The along-shore record shows a repeating and asymmetric pattern of currents synchronized with the tides. Note also the rapid reversal in the direction of the mean along-shore current at the midpoint of the flood.

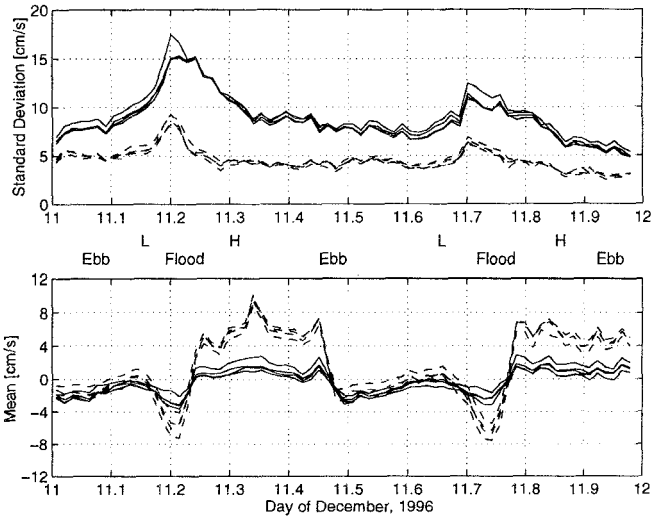

Figure 5. 20 MINUTE STANDARD DEVIATIONS AND MEANS FOR DECEMBER 11, 1996 - The two panels show the standard deviations and the means of the on-shore (—) and along-shore (– –) velocities at Levels 3, 5, 7, and 8. The nominal heights are 8.5 cm, 13.5 cm, 18.5 cm, and 21 cm above the smoothed fluid-sediment interface that existed at the beginning of the deployment. The calculations were performed on sequential 20 minute sections of the measurements. The state of the tide is marked in the strip between the two panels. The standard deviations show the sharp increase in wave velocities associated with the flood tide and also the semi-diurnal inequality of this characteristic. The means show the asymmetric along-shore flow. The combination of the on-shore and along-shore means, the known location of the measurement, and the bathymetry support the idea that vortical motion on the scale of the beach begins midway through the period of flood and persists until the midpoint of the ebb tide. Note again the rapidity of the along-shore flow reversal during the flood tide.

for December 11, a representative day. Note particularly the correlation of wave velocities with tidal phase and the asymmetry of the mean along-shore flow.

Measurements taken over the 3.5 week duration of the deployment show that the strength of the enhancement is positively correlated with the strength of the flood tide. Tidal modulation occurs on semi-diurnal, diurnal, and spring/neap time scales. The increase in near-bottom wave velocities also appears to be correlated with a decrease in wave period.

Higher wave velocities and shorter wave periods both increase the level of bottom stress. For this site, the level of bottom stress due to waves is amply sufficient to transport the 250 μm sand grains in the bed during the flood phase of the tide. Conversely, the bottom stress during the tidal ebb is not generally sufficient to initiate motion of the grains. The result is regular reworking of the sand bed on semi-diurnal, diurnal, and spring/neap time scales. Episodically, the bed was also reworked by storms. These irregular wind events produced increases of wave velocities and decreases of wave periods comparable to or greater than those produced by the tides. However, the regularity and strength of the tidal modulation, combined with the asymmetry of the mean tidal flow, suggest that this is one of the primary mechanisms controlling the evolution of Nobska Beach.

B. Vertical Structure in the Horizontal Velocity

The BASS Rake is a multiple sample volume instrument. The field prototype can measure a complete, ten height, horizontal velocity profile, extending from the bottom to 30 $cmab$, within a 6 ms window. The ability to do this in the field, reliably and autonomously, is essentially unique [6]. The measurement of a complete profiles relative to a fixed platform allows the instrument to track changes in bottom location and morphology throughout a deployment. The denser vertical spacing of acoustic axes planned for future versions of the sensor head will significantly improve the resolution of changes in bed and bedform height. Much more importantly, the nearly synchronous measurements in a BASS Rake profile make it possible to image vertically coherent structures in the flow over a range of time scales that is limited only by the sample rate and the speed and capacity of bulk data storage. Vertical coherence in the flow is inherently invisible to instruments with a single measurement volume, a category which includes most instruments capable of making measurements within a few centimeters of the bottom. BASS Rake profiles can begin within a few millimeters of the bottom [2, 5, 6].

A representative time series from the flume tests of the BASS Rake laboratory prototype is shown in Figure 6 to illustrate this point. That instrument measured the along-flume velocity at three heights above a thick bed of natural sand [5, 6]. The data shown were obtained over a smooth, level bed with a nominal fluid velocity of 8 $cm \cdot s^{-1}$ and a depth of 10 cm. Several vertically coherent velocity structures are apparent in the record. Ex-

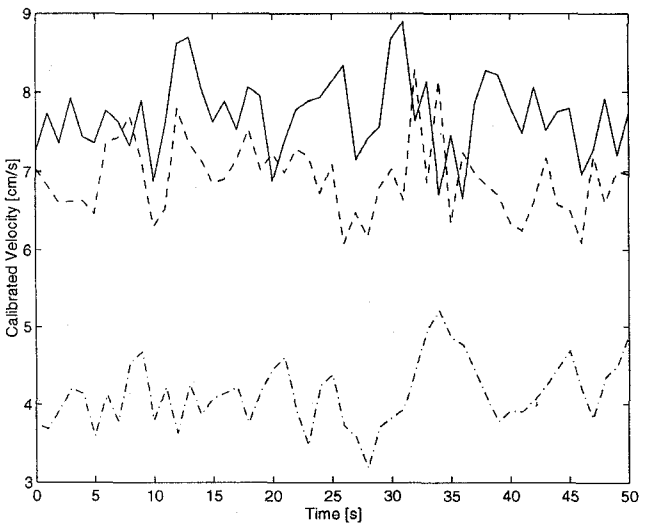

Figure 6. DETAIL FROM $8\,cm \cdot s^{-1}$ VELOCITY RECORDS - The velocity measurements at $0.45\,cmab$, $2.4\,cmab$, and $4.9\,cmab$ are denoted by $-\cdot$, $--$, and —. The concurrent velocity records at three heights in the boundary layer are able to resolve vertically coherent velocity structures and turbulent instabilities over a broad range of time scales. Several examples from the traces shown here are described in the text. Information about the dynamic behavior of the boundary layer can only be obtained by making essentially instantaneous profile measurements such as these.

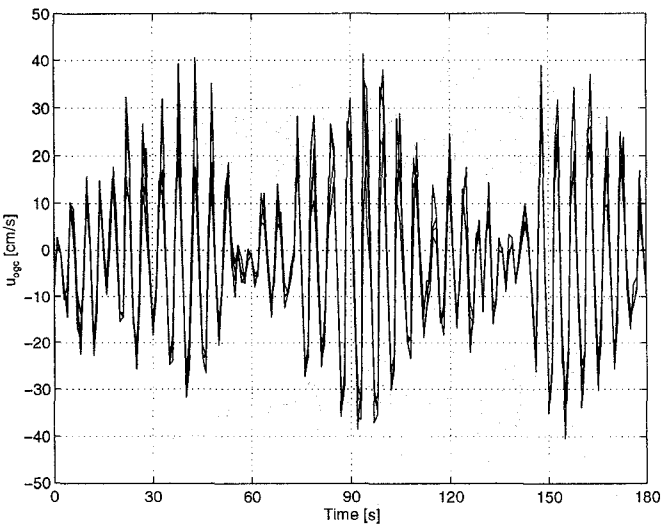

Figure 7. 3 MINUTE TIME SERIES, 0445 HOURS ON DECEMBER 11, 1996 - This is a 3 minute record of the on-shore velocity, u_{ogc}, measured at Levels 3, 5, 7, and 8. The nominal heights are $8.5\,cmab$, $13.5\,cmab$, $18.5\,cmab$, and $21\,cmab$. The time series begins at 11.20 (0445 hours) on December 11. The passage of several organized wave groups is apparent. The dominant wave period is $5\,s$. The relatively high near-bottom velocities and the short wave period result in high levels of bottom stress and modification of the sand bed.

amples of turbulent instabilities, the vertical exchange of horizontal momentum that sustains the boundary layer, are also evident.

The turbulent fluctuations evident in the figure occur on time scales of $3\,s$ to $5\,s$ and faster, with typical magnitudes of $1\,cm \cdot s^{-1}$ to $2\,cm \cdot s^{-1}$. A multi-peaked structure with both above and below average velocities and vertical coherence from $2.4\,cmab$ to $4.9\,cmab$ is visible centered at $15\,s$. The structure is preceded and followed by possible examples of bursting and sweeping, the vertical exchange of momentum in the boundary layer.[2] An apparent sweep, with vertical coherence from $0.45\,cmab$ to $2.4\,cmab$, can be seen between $8\,s$ and $10\,s$ in the velocity records. The magnitude of the sweep is large enough that the velocity at $2.4\,cmab$ briefly exceeds the $4.9\,cmab$ velocity. A possible burst at $20\,s$ occurs in the $4.9\,cmab$ velocity. Finally, a more complicated interaction is visible from $30\,s$ to $40\,s$, with a prolonged sweep in the $0.45\,cmab$ and $2.4\,cmab$ velocities and a concurrent burst in the $4.9\,cmab$ velocity. Alternatively, the record at $28\,s$ could be interpreted as a coherent burst across all three measurement levels followed by a sweep from $30\,s$ to $36\,s$ that exhibits a transport lag as it approaches the bottom. Information about the dynamic structure of the boundary layer, like this, can only be measured by an instrument with multiple sample volumes.

Returning to the field data, Figure 7 shows the propagation of several wave groups past the sensor during the first flood tide on December 11. Velocities were measured at four heights above the sand ripples then present. The short wave period and high near-bottom velocities apparent in the traces create the high levels of bottom stress responsible for the motion of sand in the bed and the reworking of the ripple field.

Sequential velocity profiles spanning a single wave cycle during ebb tide on December 11 are shown in Figure 8. The profiles show some evidence of turbulence in the flow. Variations of the profiles from smooth curves are real velocity signals, not sensor noise, and are due to the advection of turbulent eddies into the sample volume by the wave and mean components of the flow. More interestingly, the profiles exhibit a consistent outward slant with the highest velocities closest to the bottom. This pattern is caused by the acceleration of wave flow over the sand ripple that obscured the lowermost measurement levels.

Finally, Figures 9 and 10 show profiles recorded on December 7, before the late night storm raised sand ripples on the smoothed bed. The relative weakness of the flood tide wave velocities is due to both the semi-diurnal inequality and spring/neap phase of the tide. The changing shapes of the velocity profiles again show the advection of turbulent structures in the near-bottom flow through the sample volume, demonstrating the ability of the BASS Rake to image these dynamic boundary layer processes.

V. CONCLUSIONS

The field prototype was constructed to demonstrate that the BASS Rake geometry would function accurately and reliably in the field. The successful acquisition of this data set has validated both the approach and its utility, concluding this phase of the development. The next step, now underway, is the fabrication and deployment of a field capable instrument using the integrated tine design described in [2] and [6]. A nonintrusive laboratory version is also planned.

[2] Bursting refers to the transport of relatively slow fluid away from the boundary. A sweep is the injection of relatively fast fluid towards the boundary.

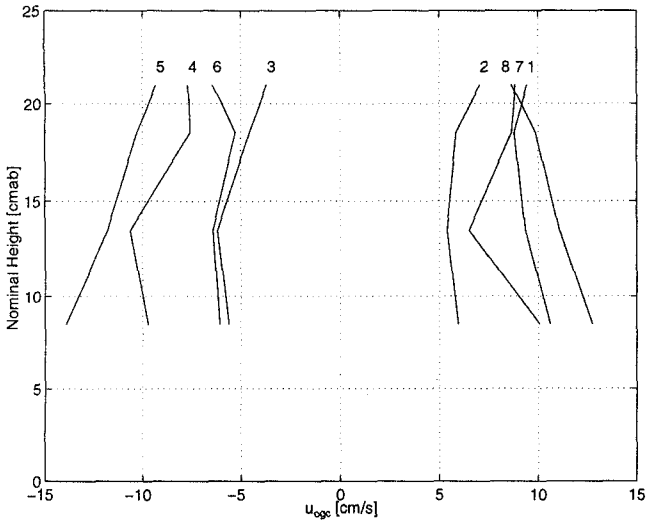

Figure 8. VELOCITY PROFILES DURING THE DECEMBER 11 EBB TIDE - The profiles are numbered in chronological sequence near the top of the figure and span approximately one wave cycle. Some effects of turbulence in the flow are visible. Note the outward slant of the profiles with the highest velocities closest to the bottom. This indicates acceleration of the flow over a sand ripple.

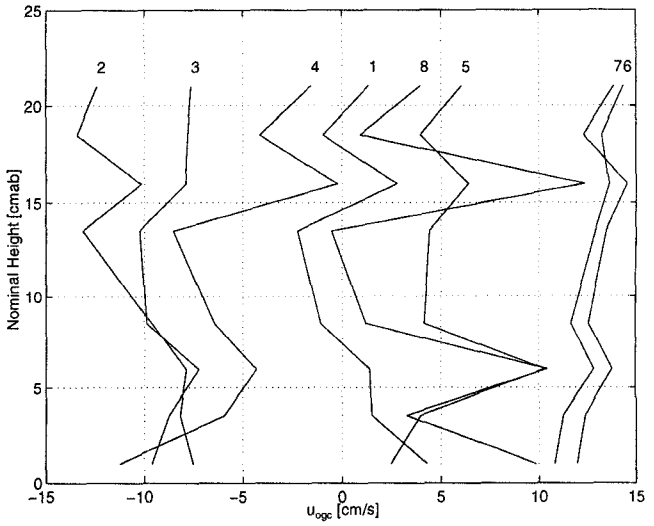

Figure 9. VELOCITY PROFILES DURING THE DECEMBER 7 FLOOD TIDE - The profiles are numbered in chronological sequence near the top of the figure and span approximately one wave cycle. Note the relatively long period, approximately 7 s, and low peak velocity. The changes in shape are caused by turbulent eddies as they are advected through the sample volume by the flow. Some of the more dramatic fluctuations are comparable to the maximum wave velocity. The steady along-shore current was $4\,cm \cdot s^{-1}$ to $6\,cm \cdot s^{-1}$ at this time. The large signal $16\,cmab$ may result from the interaction of steady along-shore and oscillatory on-shore advection. The near-bottom excursion amplitude is approximately $13\,cm$.

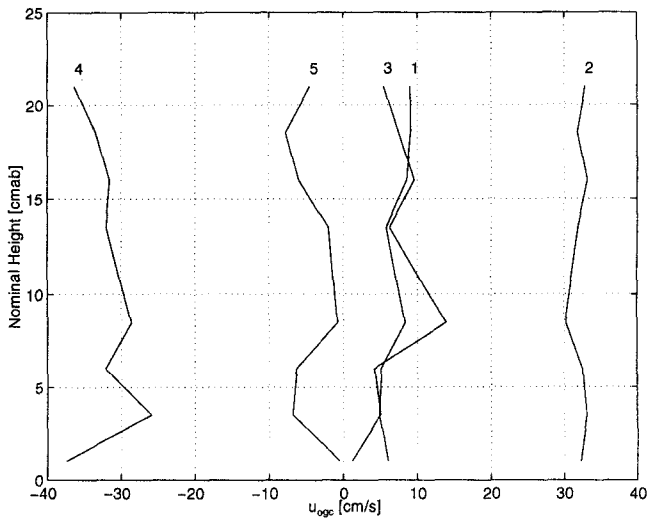

Figure 10. VELOCITY PROFILES DURING THE DECEMBER 7 STORM - The profiles are numbered in chronological sequence near the top of the figure and span approximately one wave cycle. The amplitude and frequency of the waves have increased considerably compared to earlier in the day, producing a significant enhancement of bottom stress. Shape changes indicating the presence of turbulent eddies are again present. The advection mechanism is invoked because the near-bottom velocity changes in profile 4 suggest an eddy scale of $3\,cm$ to $5\,cm$. The excursion amplitude is approximately $20\,cm$.

REFERENCES

[1] Madsen, O. S., "Sediment Transport on the Shelf", Final Draft of Chapter III.6 of The Coastal Engineering Manual, to be published by the U. S. Army Corps of Engineers, Waterways Experiment Station, Coastal Engineering Research Center, December 30, 1993.

[2] Morrison, A. T., III, "A New Technique for Detailed Acoustic Current Profiles in the Continental Shelf Wave Bottom Boundary Layer", *Proceedings of the IEEE Fifth Working Conference on Current Measurement*, IEEE/OES, February 1995, pp. 220-225.

[3] Morrison, A. T., III, "Multiplexer Design for the BASS Rake Acoustic Transducer Array", *Proceedings OCEANS '95*, MTS/IEEE/OES, October 1995, Vol. III, pp. 1528-1532.

[4] Morrison, A. T., III, "Low Impedance Multiplexer for BASS Rake Transducer Array", *Sea Technology*, May 1996, Vol. 37, No. 5, pp. 15-21.

[5] Morrison, A. T., III, Williams, A. J., 3rd, "Preliminary Tow Tank and Flume Tests of a Prototype BASS Rake Wave Bottom Boundary Layer Sensor", *Proceedings OCEANS '96*, MTS/IEEE/OES, September 1996, Vol. I, pp. 451-456.

[6] Morrison, A. T., III, Development of the BASS Rake Acoustic Current Sensor: Measuring Velocity in the Continental Shelf Wave Bottom Boundary Layer, Ph. D. thesis, Massachusettes Institute of Technology/Woods Hole Oceanographic Institution Joint Program in Oceanographic Engineering, June 1997.

[7] Williams, A. J., 3rd, Tochko, J. S., Koehler, R. L., Grant, W. D., Gross, T. F., Dunn, C. V. R., "Measurement of Turbulence in the Oceanic Bottom Boundary Layer with an Acoustic Current Meter Array", *Journal of Atmospheric and Oceanic Technology*, Vol. 4, No. 2, June 1987.